Original Article

JCBFM

Journal of Cerebral Blood Flow & Metabolism
2020, Vol. 40(8) 1658–1671

DOI: 10.1177/0271678X19872563
journals.sagepub.com/home/jcbfm
SAGE

Choroid plexus perfusion and intracranial cerebrospinal fluid changes after angiogenesis

Skylar E Johnson[1], Colin D McKnight[1], Sarah K Lants[1], Meher R Juttukonda[1], Matthew Fusco[2], Rohan Chitale[2], Paula C Donahue[3], Daniel O Claassen[4] and Manus J Donahue[1,4,5]

Abstract

Recent studies have provided evidence that cortical brain ischemia may influence choroid plexus function, and such communication may be mediated by either traditional CSF circulation pathways and/or a possible glymphatic pathway. Here we investigated the hypothesis that improvements in arterial health following neoangiogenesis alter (i) intracranial CSF volume and (ii) choroid plexus perfusion in humans. CSF and tissue volume measurements were obtained from T_1-weighted MRI, and cortical and choroid plexus perfusion were obtained from perfusion-weighted arterial spin labeling MRI, in patients with non-atherosclerotic intracranial stenosis (e.g. Moyamoya). Measurements were repeated after indirect surgical revascularization, which elicits cortical neoangiogenesis near the revascularization site ($n = 23$; age $= 41.8 \pm 13.4$ years), or in a cohort of participants at two time points without interval surgeries ($n = 10$; age $= 41.7 \pm 10.7$ years). Regression analyses were used to evaluate dependence of perfusion and volume on state (time 1 vs. 2). Post-surgery, neither CSF nor tissue volumes changed significantly. In surgical patients, cortical perfusion increased and choroid plexus perfusion decreased after surgery; in participants without surgeries, cortical perfusion reduced and choroid plexus perfusion increased between time points. Findings are discussed in the context of a homeostatic mechanism, whereby arterial health, paravascular flow, and/or ischemia can affect choroid plexus perfusion.

Keywords

Cerebrospinal fluid, choroid plexus, glymphatic, arterial spin labeling, perfusion, ischemia

Received 23 January 2019; Revised 15 July 2019; Accepted 18 July 2019

Introduction

CSF circulation is fundamental to providing immunological and mechanical protection, and indirectly contributes to autoregulatory balance via intracranial pressure maintenance.[1] The traditional model of CSF production and flow portrays CSF (i) production in the choroid plexus complexes, (ii) flow through the cerebral aqueduct and circulation through arachnoid space, and (iii) removal through arachnoid projections into the venous system.

More specifically, in humans the choroid plexus is comprised of a plexus of modified ependymal cells, which operate in coordination with the blood circulation to produce CSF (total volume = 125–150 mL;

[1]Department of Radiology and Radiological Sciences, Vanderbilt University School of Medicine, Nashville, TN, USA
[2]Department of Neurosurgery, Vanderbilt University School of Medicine, Nashville, TN, USA
[3]Department of Physical Medicine and Rehabilitation, Vanderbilt University School of Medicine, Nashville, TN, USA
[4]Department of Neurology, Vanderbilt University School of Medicine, Nashville, TN, USA
[5]Department of Psychiatry, Vanderbilt University School of Medicine, Nashville, TN, USA

Corresponding author:
Manus J Donahue, Department of Radiology and Radiological Sciences, Vanderbilt University Medical Center, Nashville, TN 37232, USA.
Email: mj.donahue@vumc.org

production rate = 20 mL/h).[2] Choroid plexus complexes are located in each of the four ventricles; however, most of the choroid plexus tissue and CSF production occurs within the lateral ventricles. The microstructure of the choroid plexus is composed of two substructures: the choroid epithelial cells and the choroid stroma. The choroid epithelial layer is comprised of a singular continuous layer of cells, derived from the ependymal lining of the ventricles. These are aligned along the basal lamina and secrete CSF along the opposite pole of the cell via villous projections. Tight junctions connecting the epithelial layer restrict the movement of substances to and from the CSF, effectively functioning as a blood–CSF barrier.[3] On the opposite side of the basal lamina resides the choroid plexus stroma. Within the stroma exists a dense vascular bed associated with blood flow four to seven times that of brain tissue. The associated capillary beds in this region contain large capillaries with thin fenestrations, thereby allowing for robust exchange of fluid and substance within the stroma.[4] The formation of CSF occurs as plasma is filtered from the blood through the network of highly vascularized epithelial cells.

Choroid plexus receives its arterial supply from the anterior choroidal artery as well as the medial and lateral posterior choroidal arteries. The anterior choroidal artery arises from the distal internal cerebral artery (ICA), superior to the origin of the posterior communicating artery. The medial and lateral posterior choroidal arteries usually arise from the P2 portion of the posterior cerebral artery (PCA), although occasionally, the medial posterior choroidal artery arises from the P1 segment of the PCA.[5] Owing to the highly vascularized nature of the choroid plexus, normative healthy choroid plexus perfusion ranges as quantified from MRI have been reported to be largely similar to gray matter perfusion in awake humans, at (mean ± standard deviation) 56 ± 21 ml/100 g/min; however, the full range can be broad at 25–90 ml/100 g/min.[6] This broad range is largely consistent with physiological expectation, as choroid plexus is well-known to respond to acute and chronic inflammatory and related stimuli, and the choroid plexus activity is highly sensitive to the brain microenvironment.[7] Furthermore, given that the arterial supply of the choroid plexus is derived from distal branches of arteries that can be easily labeled with pseudo-continuous arterial spin labeling (pCASL) MRI approaches, it is possible to quantify arterial blood water exchange at the level of the choroid plexus, a measure related to choroid plexus perfusion, using pCASL applied with typical labeling geometries that label blood water at the approximate location of the cervical ICAs (C1) and near the confluence of the vertebral and basilar arteries.

The relevance of choroid plexus function has gained increased attention recently in light of immunological and physiological studies that have provided evidence in support of a CNS lymphatic drainage system in vertebrate animals.[8–10] The potential existence of this system has expanded the description of CSF production and flow, as accumulating evidence suggests that communication exists between brain parenchyma, paravascular and interstitial spaces, and draining lymphatic vessels and cervical lymph nodes.[11] There are multiple competing theories on the role and structure of this *glymphatic system* and associated CSF clearance pathways[12–14]; however, central to most glymphatic theories is that this newly identified pathway may be central to clearance of interstitial solutes, and, in coordination with meningeal lymphatic vessels, assists with the clearance of fluid and metabolic waste products toward cervical lymph nodes. As a result, the traditional model for flow of CSF has been modified[15]; it has now been argued that CSF influx additionally occurs along *paravascular* spaces (Figure 1). Aquaporin-4 (AQP4) channels mediate the flow of fluid from the arterial paravascular space to interstitial space. Convection currents from astrocytes allow for net fluid flow through interstitial space, and fluid exits into venous paravascular space via AQP4 channels. Net fluid flow then reaches the cervical lymph nodes through small CNS lymphatic channels.

However, mechanisms of CSF circulation remain debated and controversial.[12–14] One reason for this is that it is extremely difficult to directly visualize sub-millimeter paravascular channels or choroid plexus activity directly. The majority of available techniques require intrathecal injection of exogenous contrast agents and/or studies in anesthetized animals,[16,17] and while these elegant studies have been fundamental to elucidating CSF circulation physiology, they are prone to the caveats that anesthesia may confound measurements and exogenous agents alter flow kinetics.

Another avenue for investigation is to evaluate at a broader level whether changes in choroid plexus perfusion and/or intracranial CSF occur following surgical improvements in arterial health. For instance, choroid plexus perfusion can be evaluated in sequence with intracranial CSF volume using non-invasive pCASL and T_1-weighted MRI, respectively. Following surgical arterio-synangiosis procedures, arterial density and blood flow can increase. The objective of this study was to quantify choroid plexus perfusion, cortical perfusion, and CSF intracranial volume before and after surgically induced neoangiogenesis in patients with intracranial stenosis. Findings are discussed in the context of different potential glymphatic and/or other feedback mechanisms relating arterial health and choroid plexus perfusion.

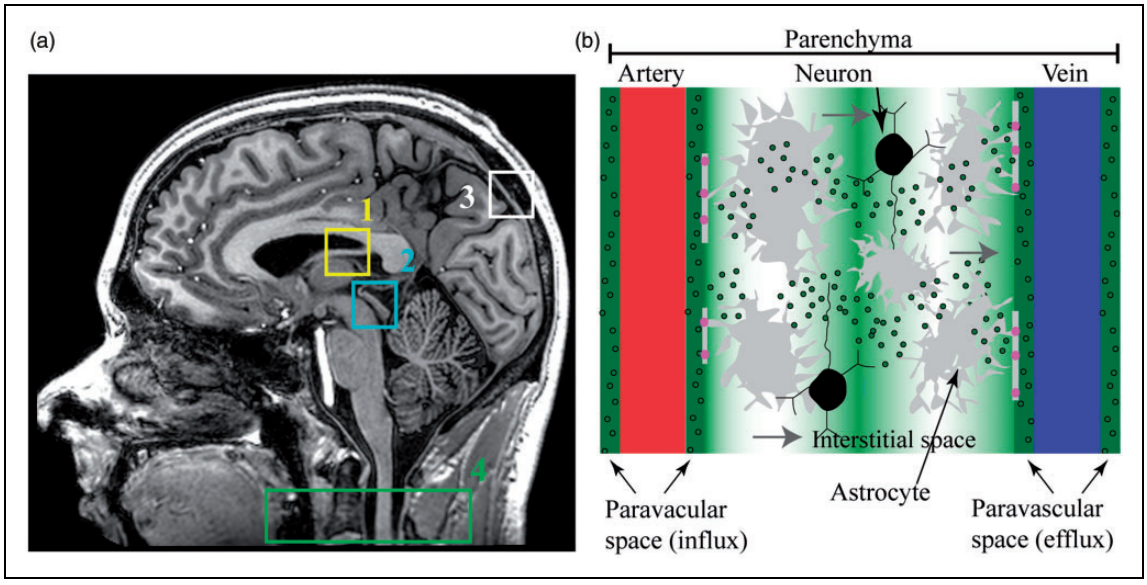

Figure 1. Components of traditional and novel CSF circulation pathways. (a) Sagittal T_1-weighted MRI showing the traditional cerebrospinal fluid (CSF) flow pathway consisting of (1) choroid plexus, which produces CSF; (2) cerebral aqueduct through which CSF flows from third to fourth ventricles, after which CSF circulates through arachnoid space where it can be (3) removed through arachnoid projections into the venous system. This system has been adapted to include (b) a glymphatic pathway, in which CSF influx occurs along periarterial spaces. Aquaporin-4 (AQP4) channels (pink) mediate the flow of fluid from the paravascular arterial space to interstitial space. Convection currents from astrocytes allow for net fluid flow through interstitial space and via AQP4 channels fluid flows into venous paravascular space. Net fluid flow reaches the cervical lymph nodes (a; 4) through small CNS lymphatic channels.

Materials and methods

Demographics and study design

All study procedures were approved by the Vanderbilt University Institutional Review Board. Participants ($n = 33$) with moyamoya disease or syndrome presenting to the neurology and/or neurological surgery services at Vanderbilt University Medical Center between 2011 and 2016 were enrolled, and all patients provided informed, written consent. All components of this study were performed in compliance with the Declaration of Helsinki of 1975 (and as revised in 1983), Health Insurance Portability and Accountability Act, and all protocols were approved by the Vanderbilt University Institutional Review Board (IRB Study 110468 or 160478). This study represents a retrospective analysis of data acquired for a separate prospective study of stroke risk in these patients.

Moyamoya disease is a non-atherosclerotic cerebrovascular condition with progressive narrowing of the intracranial arteries (primarily intracranial internal carotid arteries, as well as middle cerebral arteries and proximal branches), and surgical revascularization can be clinically indicated in this population or in patients with moyamoya syndrome (secondary to a separate condition such as atherosclerosis or sickle cell anemia) when steno-occlusion becomes severe or ischemic neurological symptoms are present.[18–20] The majority of these patients ($n = 23$) were scheduled for indirect surgical revascularization and all received a multi-modal MRI protocol before and after surgical revascularization. All revascularizations were clinically indicated and of indirect synangiosis type including encephaloduroarteriosynangiosis or encephaloduroarteriomyosynangiosis (Table 1). In addition, to allow for a comparison of the stability of functional and tissue volume measures in this population, moyamoya patients ($n = 10$) without any interval intervention were scanned twice with a similar interval scan duration. While it is well-known that moyamoya can be progressive over this period, this cohort was intended to provide an approximate reference of parameter stability in a similar disease cohort matched for age and sex as the intervention cohort. The non-surgical cohort is deliberately not representative of a healthy cohort in whom perfusion parameters are already well-known from the literature and have recently been reviewed.[21]

Imaging and angiography procedures

Two scans were performed in each participant using a non-contrast 3 Tesla (Philips Achieva, Best, The Netherlands) head MRI protocol with body coil radiofrequency transmission and 16-channel SENSE-array

Table 1. Demographics for surgical (above) and non-surgical (below) patients.

	Age (years)	Race (percent Asian)	Sex (percent female)	Time from surgery to follow-up scan (days)	Fraction idiopathic
Surgical ($n = 23$)					
MEAN ± STD	41.8 ± 13.4	13.0	86.5	275.1 ± 134.2	0.739
Non-surgical ($n = 10$)					
MEAN ± STD	41.7 ± 10.7	20.0	90.0	359.5 ± 236.2	0.800

Note: In patients that were not idiopathic moyamoya, atherosclerosis was the believed relevant co-morbidity in all cases, and the dominant race in both groups was Caucasian. All participants were symptomatic with history of transient ischemic attack or stroke and no subjects had sickle cell anemia, Down's syndrome, or neurofibromatosis. In surgical patients, the initial scan occurred within 30 days of surgery, and as such, the time from surgery to follow-up can be interpreted analogously as the scan interval listed for the non-surgical patients within this range.
STD: standard deviation.

reception. The anatomical imaging protocol consisted of (i) T_1-weighted magnetization-prepared-rapid-gradient-echo (spatial resolution $= 1 \times 1 \times 1\,mm^3$), (ii) T_2-weighted fluid-attenuated-inversion-recovery (FLAIR; 2D turbo-spin-echo; spatial resolution $= 0.9 \times 0.9 \times 4\,mm^3$), (iii) T_2-weighted (2D turbo-spin-echo; spatial resolution $= 0.9 \times 0.9 \times 3\,mm^3$), and (iv) diffusion-weighted imaging ($b = 0$ and $b = 1000\,s/mm^2$; spatial resolution $= 1.1 \times 1.1 \times 4\,mm^3$). Non-contrast time-of-flight head and neck magnetic resonance angiography (MRA) were performed if digital subtraction angiography was unavailable within 30 days of MRI. The purpose of angiography was to confirm the diagnosis of moyamoya as well as to guide revascularization candidacy, but these data were not used for testing study hypotheses directly.

The anatomical imaging protocol was complemented with perfusion-weighted pseudocontinuous arterial spin labeling (pCASL).[22] Perfusion is tightly coupled to glucose metabolism[23] and provides a non-invasive surrogate of tissue function and vascular health that can be more informative and quantitative than T_2*-weighted blood oxygenation level-dependent (BOLD) contrast alone, especially in patients with cerebrovascular disease.[24,25] Arterial blood water was magnetically labeled using a long (duration = 1550 ms) string of short (0.5 ms) Hanning-windowed block radiofrequency pulses, followed by a 2D echoplanar imaging readout with spatial resolution $= 3 \times 3 \times 7\,mm^3$. A post-labeling delay (post-labeling delay = 1550 ms) was included to allow the labeled blood water to flow into the imaging slice, exchange with tissue water, and attenuate the extravascular water signal. The extent of attenuation can be quantified by comparing the labeled image to an image in which blood water is not labeled. This difference magnetization map can be normalized by an equilibrium magnetization image, obtained with identical geometry and readout but with long repetition time = 15 s and spin labeling removed, to enable perfusion quantitation in absolute units (mL blood/100 g tissue/min). In moyamoya patients with delayed blood arrival, pCASL can also suffer from contamination from endovascular signal[26,27] and the relevance of this effect is addressed in the *Discussion* as well as in the literature.[26–28]

Analysis

The presence of interim (i.e. between scan) infarcts was evaluated by a board-certified radiologist as new ischemic lesions ≥ 3 mm in diameter[29,30] using established criteria of hyperintense on T_2-weighted FLAIR and hypointense on T_1-weighted imaging approaching CSF signal.[30]

For volumetric determination, T_1-weighted scans were segmented using a standard procedure consisting of a hidden Markov random field model and an associated expectation-maximization algorithm,[31] and images were segmented into the three tissue types: (i) CSF, (ii) gray matter, and (iii) white matter using a 75th percentile probability threshold. The total intracranial volume was calculated as the sum of these three tissue types, and the total non-fluid tissue volume was calculated as the sum of gray matter and white matter volumes. Tissue volumes are reported in mL.

For perfusion determination, pCASL data were corrected for motion and slice-time delay in the 2D echoplanar imaging readout (slice acquisition time = 23 ms), surround-subtracted, normalized by equilibrium magnetization, and voxel-wise perfusion maps were calculated upon application of the simplified International Society for Magnetic Resonance in Medicine perfusion study group model.[32] We used the same kinetic model and partition coefficient (0.9 ml/g) for calculating choroid plexus perfusion as we did for calculating cortical perfusion, as has been done in an earlier study of choroid plexus perfusion using ASL MRI.[6] Subject

equilibrium (M_0) images were co-registered to the participant's T_1-weighted image, which was subsequently co-registered to a 4 mm T_1-weighted Montreal Neurological Institute atlas.[33] A 4 mm atlas was used rather than a 2 mm atlas as the 4 mm atlas most closely resembles the nominal spatial resolution of the pCASL scan. The transformation matrix was then applied to the quantitative perfusion map to move the perfusion map into the T_1-weighted space and subsequently into standard space. The choroid plexus is visible on the T_1-weighted scans, and perfusion was quantified in the choroid plexus located within the atrium of the lateral ventricles, separately in the right and left hemispheres. The volume of the choroid plexus region was approximately 3 mL. Cortical perfusion was calculated near the surgical resection site spanning a volume of approximately 30 mL.

Statistical procedures and considerations

The primary objective of this study was to test the hypothesis that intracranial CSF volume and choroid plexus perfusion change after improving arterial flow and associated arterial paravascular flow with a surgical anastomosis procedure. In evaluating this objective, we sought to understand whether any changes in the measured CSF properties were associated with (i) choroid plexus perfusion measured from arterial spin labeling MRI or (ii) cortical parenchymal perfusion measured from arterial spin labeling MRI in cortical regions near the revascularization site. Means, standard deviations, and ranges of continuous parameters were calculated, along with frequencies and ranges for categorical variables. In all regression analyses, model coefficients, standard error, p-values, and 95% confidence intervals are reported.

First, to evaluate whether CSF or tissue volume changed before vs. after surgical revascularization, a Wilcoxon signed-rank test was applied to the total intracranial CSF volume or tissue volume for all participants with interval surgeries before vs. after the surgical revascularization. To gain additional information on the normal range of volume changes in this population over time, an identical analysis was applied to participants without interval surgeries. This preliminary analysis yielded two comparisons for each group, and a Bonferroni corrected p-value of 0.025 was required for significance.

We also sought to understand whether revascularization surgery was associated with a change in either the (i) cortical perfusion or (ii) choroid plexus perfusion. Here, a logistic regression analysis was performed across all 33 participants (23 with interval surgeries and 10 without) using the participant category (interval surgery vs. no interval surgery) as the dependent variable and cortical perfusion change, choroid plexus perfusion change, and interval scan time as the dependent variables. Criterion for significance was two-sided $p \leq 0.05$.

Data availability

De-identified data and data processing scripts will be made available to others with human subjects Collaborative Institutional Training Initiative training for purposes of reproducing the study findings.

Results

Participant demographics are summarized in Table 1, including for the cohort with ($n = 23$; age $= 41.8 \pm 13.4$ years; sex $= 87\%$ female) and without ($n = 10$; age $= 41.7 \pm 10.7$ years; sex $= 90.0\%$ female) interval surgeries. In surgical patients, the duration from surgery to post-surgical imaging was 275 ± 134.2 days. This duration was allowed to provide time for neoangiogenesis, which generally occurs over a period of 6–12 months. The interval time between scans in the participants without interval surgeries was 360 ± 236.2 days. No participants had interval overt strokes between scans.

An angiogram obtained from a representative participant (age = 32 years; gender = female) scanned pre- and post-revascularization is shown in Figure 2, which highlights the potential impact of these surgeries on new vessel growth. In participants without interval surgeries, the intracranial CSF volume (360.5 ± 34.1 mL) and total tissue volume (1287.8 ± 81.2 mL) at the first time point were statistically unchanged from the intracranial CSF volume (356.7 ± 23.9 mL) and total tissue volume (1254.8 ± 107.2 mL) at the second time point. In participants with interval surgeries as well, the intracranial CSF volume (367.6 ± 45.0 mL) and total tissue volume (1349.3 ± 114.3 mL) at the first time point (pre-surgical) were statistically unchanged from the intracranial CSF volume (372.8 ± 44.7) and total tissue volume (1324.0 ± 122.7 mL) at the post-surgical time point. Note that the CSF volumes observed here are slightly larger than brain CSF volumes as the T_1-weighted image placement extended to the junction of the second and third vertebrae and therefore contains some CSF surrounding the spinal cord as well. These data are consistent with neither the total tissue volumes nor total CSF volumes changing significantly before versus after surgery or at two time points in the non-surgical cohort. The two-sided p-value for the CSF volume change was 0.10 and for the tissue volume change was 0.52. A lack of significant changes in these volumes is consistent with the Monro–Kellie hypothesis[34]; however, it should be noted that we did observe a trend ($p = 0.10$) for a change in CSF volume.

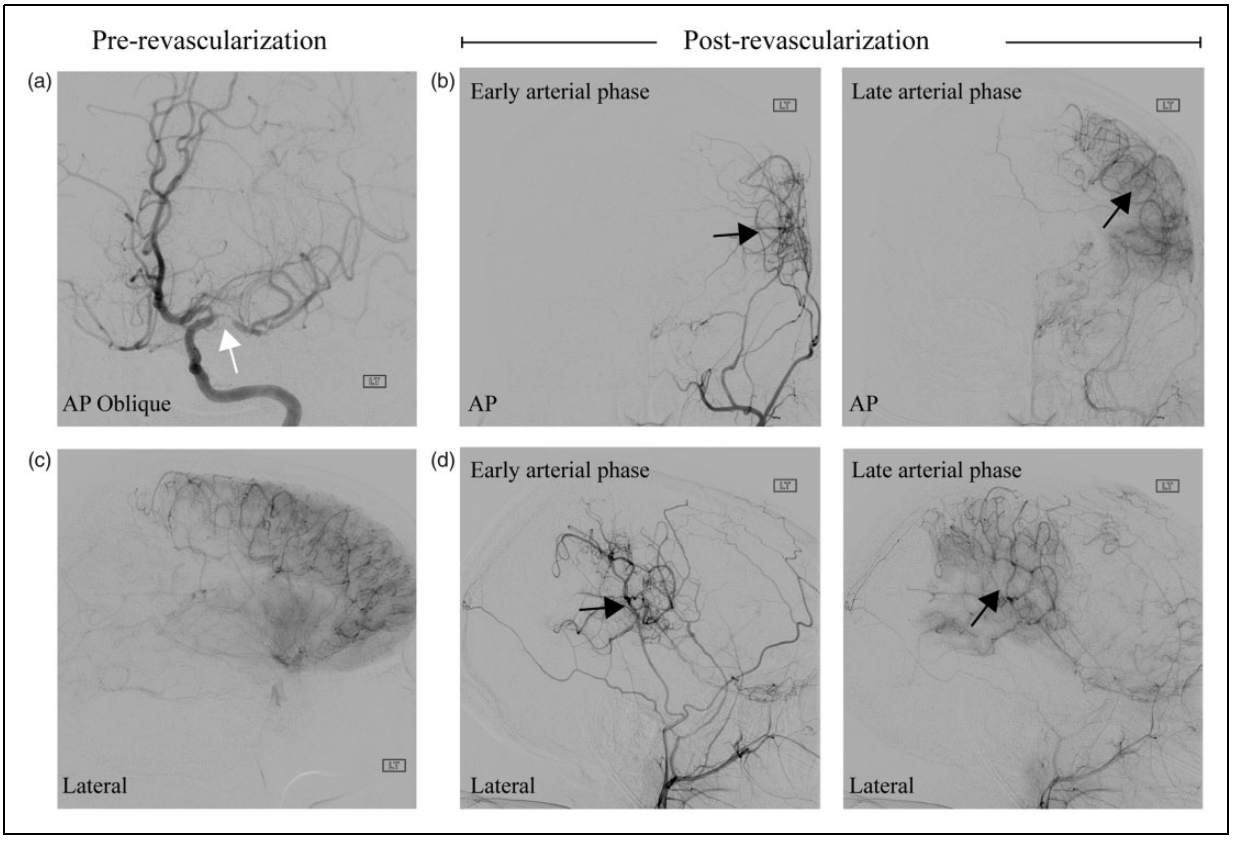

Figure 2. Indirect surgical revascularization. A 32-year-female patient scanned before and after an encephaloduroarteriosynangiosis indirect surgical revascularization. (a) Anterior–posterior oblique projection following injection of the left internal carotid artery shows clear middle cerebral artery stenosis (white arrow) and limited middle cerebral artery territory filling. (b) Post-revascularization and following left external carotid artery injection, neoangiogenesis and increased collateralization (black arrows) are apparent in both the early (left) and late (right) arterial lateral projections. (c) Shows the pretreatment lateral projection following left internal carotid artery injection in late arterial phase, which shows large areas of poor arterial supply to portions of the right middle cerebral artery distribution and (d) The lateral correlate of panel (b).

On average, the cortical perfusion reduced in participants without interval surgeries from 41.7 ± 20.7 mL/100 g/min to 34.8 ± 11.4 mL/100 g/min (16.5% decrease) and the choroid plexus perfusion increased from 37.9 ± 10.7 mL/100 g/min to 41.1 ± 14.2 mL/100 g/min (8.6% increase). The opposite trend was observed in the participants with interval surgeries, in which the cortical perfusion on the side of revascularization increased from 45.8 ± 17.8 mL/100 g/min to 48.5 ± 20.1 ml/100 g/min (5.8% increase) and the choroid plexus perfusion reduced from 47.3 ± 14.7 ml/100 g/min to 42.1 ± 12.6 mL/100 g/min (10.9% decrease) (Figure 3). It is reasonable that the large inter-subject variation in metrics is associated with variation in the revascularization success and time between scans, and this possibility was analyzed here as well. When these changes were considered in a logistic regression, which investigated the dependence of group (dependent variable; interval surgery or not) on cortical perfusion change (indicative of collateralization growth and revascularization success[35]), choroid plexus perfusion change, and interval scan duration, it was found that the choroid plexus perfusion change ($p = 0.035$), and interval time ($p = 0.031$) were both significantly related to the group (surgical or non-surgical), and a strong trend ($p = 0.051$) for cortical perfusion change was observed. These data are consistent with cortical perfusion near the surgical revascularization site increasing by more in patients undergoing surgical revascularization, as expected, but also the choroid plexus perfusion reducing in patients undergoing surgical revascularization, and these trends depend on the time since surgical revascularization.

Case examples summarizing mean effects are shown in Figure 4.

Discussion

We investigated how intracranial CSF volume, choroid plexus perfusion, and cortical perfusion adjust in

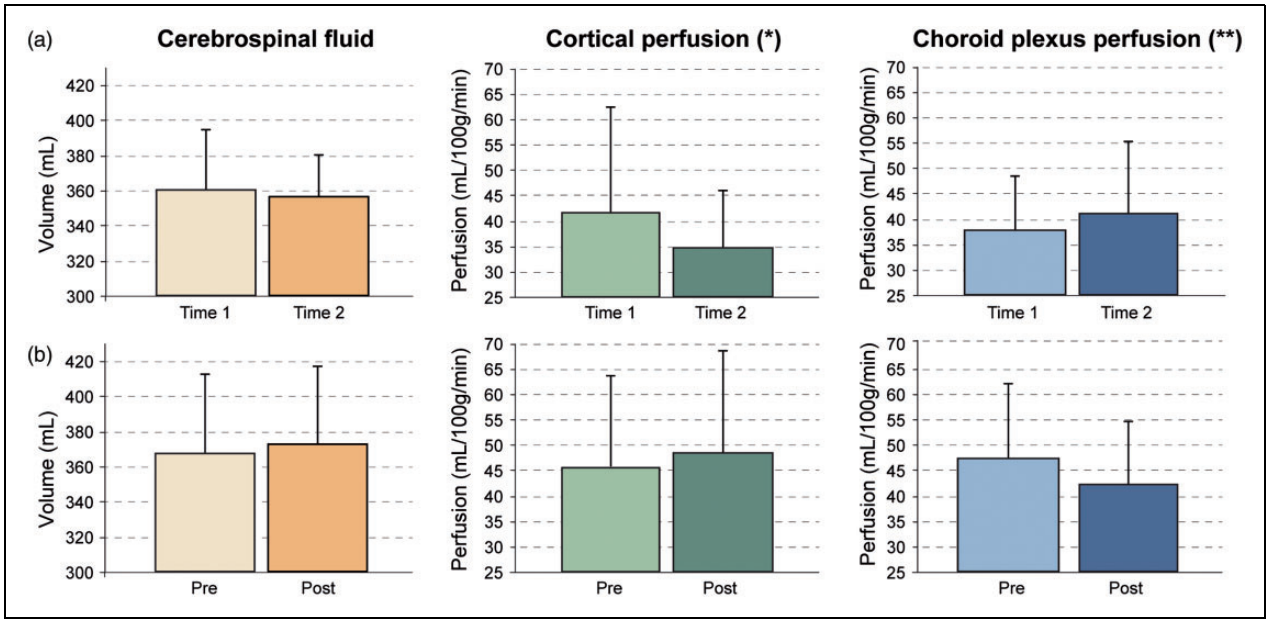

Figure 3. Group-level relationships between study parameters. Cerebrospinal fluid (CSF) volume, cortical perfusion near the revascularization site, and choroid plexus perfusion in (a) non-surgical participants scanned at two time points and (b) surgical participants scanned before and after revascularization. In both groups, CSF volume does not change significantly. However, in the non-surgical group (a), cortical perfusion decreases slightly and choroid plexus perfusion increases slightly. Alternatively, in the surgical group (b), the cortical perfusion increases slightly, consistent with the effect of revascularization, and the choroid plexus perfusion decreases. Error bars denote standard deviation and summarize the large inter-subject variation, consistent with known, varied responses of surgical revascularization and the heterogeneous and varied nature of the disease. Significance of these findings are reported in the regression analysis in Table 2, in which a strong trend ($*p = 0.05$) is found for the cortical perfusion change between times for the different groups, and a significant ($**p = 0.035$) choroid plexus perfusion change is found between times for the different groups, after accounting for interval scan duration.

Table 2. Results of the logistic regression analysis using group as the dependent variable (e.g. interval surgery or no interval surgery) and (i) cortical perfusion change, (ii) choroid plexus perfusion change, and (iii) interval scan duration as the explanatory variables.

	Coefficients	Standard error	t-stat	*p*-value	Lower 95%	Upper 95%
Intercept	0.968	0.155	6.241	<0.001	0.651	1.287
Cortical perfusion change	0.485	0.238	2.035	0.051	−0.003	0.973
Choroid plexus perfusion change	−0.577	0.261	−2.214	0.035	−1.110	−0.043
Interval scan duration	−0.001	0.001	−2.183	0.031	−0.002	0.000

Note: Note that as the surgery occurred within 30 days of the first scan, the interval scan duration is an approximate indicator of the time after the revascularization surgery in the surgical cohort. The model F-statistic was 3.455 and associated F-significance was 0.0297. These results suggest that the change in both the cortical perfusion and choroid plexus perfusion is significantly related to whether the participant had an interval surgery or not, and that the changes in these parameters, as indicated by the coefficients, are in opposite directions for the two groups (see Figure 4 for representative cases).

moyamoya participants following an indirect surgical revascularization procedure, which should reduce ischemia and improve arterial health (and possibly associated paravascular flow). We found that intracranial CSF and tissue volumes did not change significantly either in surgical or non-surgical participants over a similar interval duration; however, in participants with interval surgeries, on average cortical perfusion near the revascularization site increased as expected and choroid plexus perfusion reduced, and the opposite finding was observed in participants without interval surgeries.

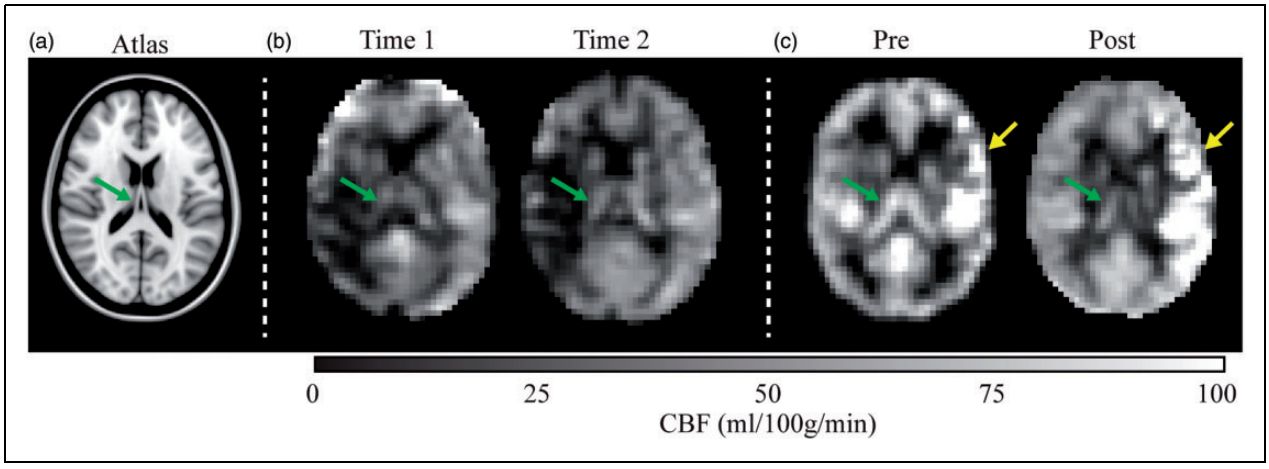

Figure 4. Longitudinal cerebral blood flow changes in two representative patients. (a) A T_1-weighted atlas at the approximate location of the shown blood flow maps. (b) A patient with moyamoya (age = 58 years; sex = female) scanned at an interval of 72 days with no interim surgery. The images suggest subtle reductions in cortical perfusion and slight increases in choroid plexus perfusion (green arrow). (c) A patient with moyamoya with interval surgery (age = 31 years; sex = female) scanned 72 days after left-sided encephaloduroarteriomyosynangiosis. Increases in cortical perfusion are observed near the revascularization site (yellow arrow), whereas bilateral decreases in choroid plexus perfusion are observed.

CSF circulation physiology

These findings should be considered after reviewing the classical understanding of CSF production in the choroid plexus complexes and subsequent circulation. Briefly, the choroid plexus consists of a network of blood vessels encased by ependymal cells that work together to ensure support and protection of the brain. Residing in the pia mater layer of the meninges, choroid plexus structures are found in both lateral ventricles, the third ventricle, and the fourth ventricle. The choroid plexus structures that reside within the ventricles, along with neighboring ependymal cells, work to produce CSF. CSF consists of water and other elements from the blood that have been filtered out of the capillaries through the ependymal layer into the cerebral ventricles. This fluid fills the cerebral ventricles, the subarachnoid space of the meninges, and the central canal of the spinal cord. One physiologic benefit of this fluid is to provide a cushion to the adjacent brain and spine parenchyma, thus assisting in mechanical stability. CSF also plays a central role in providing nutrients to the adjacent brain and spine and allows for efficient removal of waste products. In addition to facilitating the production of CSF, the choroid plexus assists in regulating the composition of the CSF through maintaining a semipermeable barrier between blood in the capillaries and CSF. In conjunction with the blood–brain barrier, the blood–CSF barrier blocks harmful elements from entering the CSF and allows helpful elements to pass through; these helpful elements include immune cells such as macrophages, lymphocytes, and microglia, which all work to prohibit pathogens from entering the brain and disrupting nervous system function. The choroid plexus, alongside the arachnoid membrane meninges, is vital in maintaining the blood–CSF barrier and thus maintaining proper central nervous system function and development.

The findings of this study, namely that choroid plexus perfusion responds to changes in surgically induced vascular health elsewhere in the cerebrum, can be interpreted in the context of the recently proposed glymphatic hypothesis; however, other explanations in terms of biochemical feedback and/or vascular contributors should also be considered as outlined below.

Glymphatic flow interpretation

Following production, there is flow of CSF through the cerebral aqueduct as well as the foramen of magendie and luschka, after which CSF circulates over the dura mater and can be absorbed into the dural venous sinuses via granular projections. This system is being reevaluated in the context of an increasingly well-characterized system of glymphatic flow. CSF flow has now been proposed to additionally include CSF movement along arterial paravascular spaces, after which fluid moves into interstitial space via AQP4 channels, and subsequently enters the venous paravascular spaces also through what are believed to be AQP4 channels (Figure 1). This paravenous fluid then possibly drains to meningeal lymphatics and cervical lymph nodes, though none of these processes have been fully articulated. The more robust interaction of fluid within the subarachnoid space and within brain parenchyma as characterized by the glymphatic system offers an intriguing new mechanism by which more complex

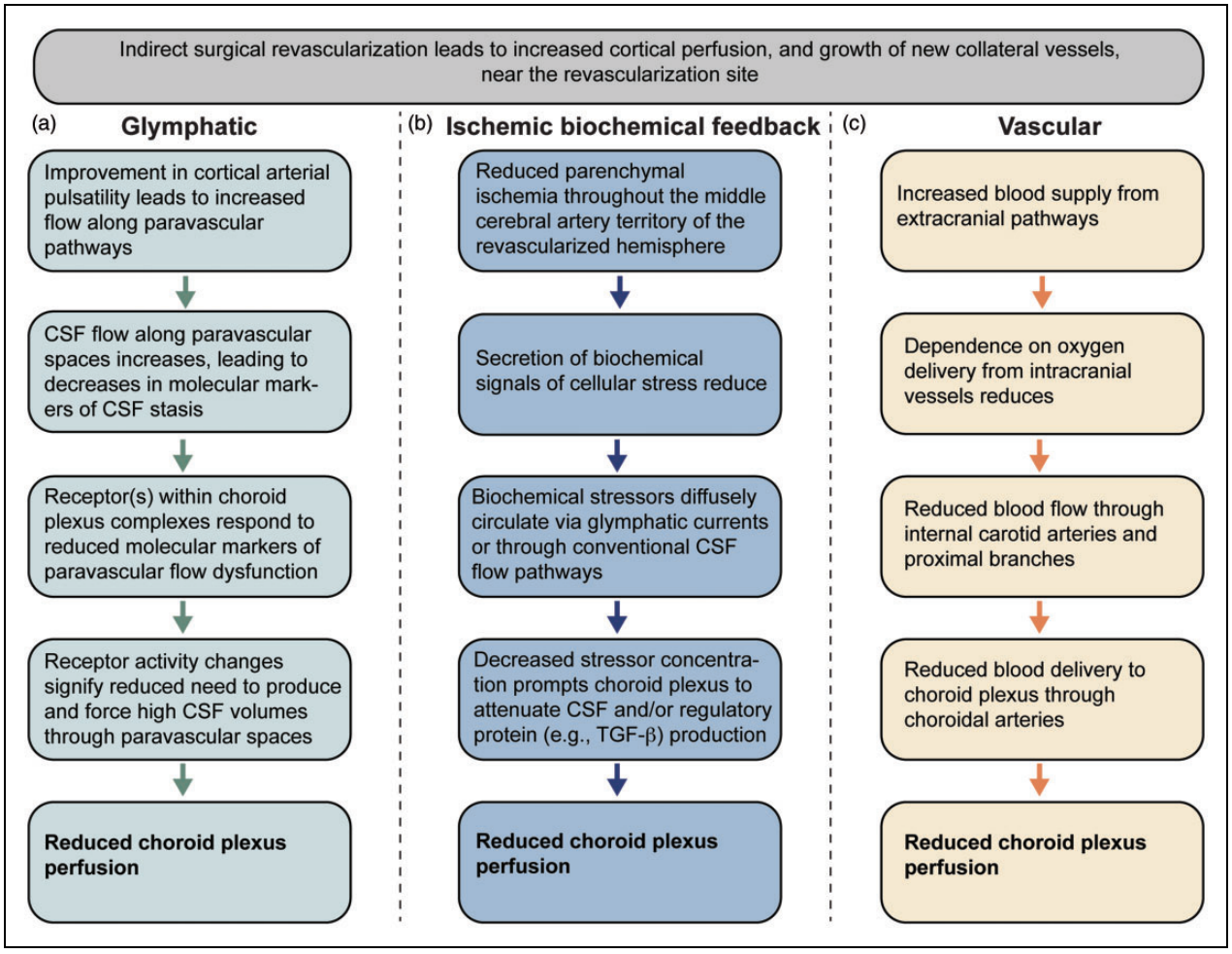

Figure 5. Hypothesized feedback mechanisms between cortical arterial health and choroid plexus perfusion. Indirect surgical revascularization on average was found to lead to increases in cortical perfusion and reductions in choroid plexus perfusion in patients with intracranial arterial steno-occlusive disease. Three possible pathways that could describe the choroid plexus perfusion reduction are proposed, which rely on (a) glymphatic, (b) ischemic biochemical feedback, and/or (c) changes in blood vasculature. It should be noted that the ischemic biochemical feedback and glymphatic pathways may share overlapping mechanisms, depending on how biochemical stressors are circulated to CSF and choroid plexus. Additional information on each pathway is provided in the Discussion.

biochemical signaling can occur between the brain parenchyma, the subarachnoid space, and the choroid plexus (Figure 5).

We observed that neither tissue nor CSF volumes change after surgical revascularization, but the perfusion of the choroid plexus does change significantly on average. We observed that the choroid plexus perfusion increased on average over approximately one year in participants not undergoing surgical revascularization, whereas the choroid plexus perfusion reduced in participants following surgical revascularization. Importantly, the directionality of these changes was in the opposite direction of the change in perfusion in the cortical regions at the location of the revascularization site, indicating that this was not a simple downstream hemodynamic effect of changing cerebral perfusion pressure only.

These data illuminate a potentially very important interplay between the cerebral arterial viability and CSF production by the choroid plexus. Findings suggest that choroid plexus perfusion may be highest when arterial health and possibly arterial paravascular flow is lowest in ischemic patients. This suggests the intriguing possibility that a feedback loop is present that allows for upregulation of choroid plexus CSF production in the setting of poor paravascular flow. In such settings where glymphatic CSF to interstitial flow is compromised, added CSF production may serve to compensate and drive glymphatic clearance of waste products from the interstitial space. Our data indicate that following revascularization and likely improvement in arterial paravascular flow secondary to increased arterial density and perhaps improved pulsatility, the choroid plexus perfusion reduces. This could reflect a homeostatic

mechanism where improved paravascular flow and more robust waste clearance prompts decreased choroid plexus CSF production. It is important to note that while this finding met the stated significance criteria, the overall detected significance may be reduced owing to the small and localized improvement of paravascular flow near the revascularization site, whereas the choroid plexus supplies CSF to the entire brain.

Further work is needed to understand what biochemical signaling methods drive this relationship and the mechanism by which increased CSF production could alter CSF to interstitial flow. Such studies would likely involve additional quantitative measurements of CSF flow velocity and local CSF volume changes, ideally paired with more direct measures of glymphatic flow which could be obtained through intrathecal injection of paramagnetic contrast agents, as has recently been shown to be feasible in humans.[36]

Alternative biochemical feedback mechanism

It is also important to note that elaborate biochemical feedback mechanisms related to neurological stressors, including those relevant to ischemia, are also in place to regulate CSF production volume and choroid plexus activity generally. The choroid plexus is known to secrete various compounds (i.e. growth factors) which are likely involved in maintaining the health of the brain parenchyma.[3] Specifically in terms of cerebral ischemia, transforming growth factor (TGF)-β, a well-known regulatory protein involved in tissue homeostasis and immune regulation, is expressed in the choroid plexus and has been reported to be elevated during ischemia in rats,[37,38] and it has been argued that regulation of TGF-β in the choroid plexus may have relevance to ensuring Ca++ homeostasis and the expression of Bcl2 proto-oncogene, a regulatory protein central to cell death, even when the ischemia is spatially removed from the choroid plexus.[39,40] As such, choroid plexus activity as related specifically to growth factor expression can be modulated by ischemia (Figure 5). There is compelling evidence that these compounds, and specifically TGF-β, play a positive role in neuronal survival and recovery of function following ischemia. Furthermore, it is logical that choroid plexus activity could be modulated directly as a result of changes in ischemia and parenchymal need for increased or decreased growth factor expression, which could also explain the change in choroid plexus perfusion observed here. Improved arterial supply to damaged or at-risk glial tissue could prompt reduced secretion of biochemical signals of cellular stress. In such a scenario, biochemical signals of stress diffusely circulated by glymphatic currents or other mechanisms would be decreased. A decrease in such signaling could prompt the choroid plexus to attenuate high CSF production levels which were previously necessary to support glial health in times of vascular stress.

Further, evaluating this possibility would be feasible in humans by applying the above measures of glymphatic flow, in combination with CSF or blood markers of these relevant growth factors.

Alternative vascular explanation

Another explanation to consider pertains to a more simple and vascular response of the choroid plexus to the revascularization. For instance, following improvement in cortical perfusion via an indirect revascularization of a distal branch of the external carotid artery to the brain tissue, there may be less demand on the intracranial vasculature to supply blood to tissue. In this case, flow through the intracranial anterior and posterior circulation may reduce, and as the choroid plexus is perfused by branches of these vessels (i.e. anterior and posterior choroidal arteries), flow to the choroid plexus could reduce as well (Figure 5). Unfortunately, in this study we did not measure quantitative flow velocities in these vessels; however, work using ultrasonography of internal and external carotid arteries following encephaloduroarteriosynangiosis in 15 pediatric moyamoya patients showed increases in peak systolic velocity in both intracranial and extracranial arteries 3–12 months after surgery, inconsistent with the above explanation.[41] In a separate study of 21 moyamoya patients pre- and post- indirect revascularization, it was observed that in poor responders, defined as a lack of collateralization apparent on post-operative angiography, the velocity changes in the superficial temporal artery as measured by ultrasonography were non-significant compared to those with more robust collateral formation, in whom flow velocities increased.[42] In this latter study, intracranial vessel velocities were not reported however. In a similar cohort of patients monitored with catheter angiography pre/post indirect revascularization at our center, we observed that in most patients at least 1/3 of the MCA territory was revascularized after approximately one year; however, the range of revascularization was variable with the majority (75%) showing at least 1/3 of the MCA territory revascularized approximately one year after surgery, with only 5% of those evaluated showing no detectable change in collateralization on catheter angiography.[35] These data collectively suggest that velocities in both intracranial and extracranial vessels increase following indirect revascularization, and therefore the possibility of flow velocity reducing following this procedure is not necessarily supported by literature. However, as we did not measure these velocities here, and also as there is evidence that the

change in flow velocity can be dependent on the robustness of collateral formation, we cannot rule out that this vascular explanation may be relevant to some patients.

Further understanding of this possibility would simply involve quantitative measurements of intracranial and extracranial flow velocities along with blood volume[43,44] before and after revascularization, potentially in patients with indirect revascularization (where new vessels and paravascular health may improve) compared to more simple direct surgical revascularization (e.g. carotid endarterectomy or middle cerebral artery bypass), where ischemia may reduce but large paravascular networks may remain unchanged.

Relationship between choroid plexus perfusion and CSF production

It should be noted that there is some controversy in the animal literature regarding how closely choroid plexus perfusion relates to CSF production.

In support of a direct relationship, when CSF production was evaluated in chloralose-anthesthetized rabbits before and after administration of angiotensin II (100 ng/kg/min), a potent vasoconstrictor, it was observed that CSF production reduced by $24 \pm 3\%$, consistent with choroid plexus perfusion being related to CSF production.[45] A relationship between choroid plexus perfusion and CSF production was also observed in a separate study of anesthetized rabbits, in which intravenous infusion of vasopressin decreased blood flow to the choroid plexus by 50–60% for the entire 90 period of infusion and also decreased CSF production by $35 \pm 8\%$.[46]

However, when using separate vasoactive stimuli other studies have found an apparent uncoupling between choroid plexus perfusion and CSF production activity. For instance, in anesthetized rabbits administered atriopeptin, a protein hormone secreted by cardiac cells and potent vasodilator, increased blood flow to the choroid plexus was observed, yet no significant or only a small effect on CSF production was observed.[47] Using laser-Doppler flowmetry during ventriculocisternal perfusion with inulin-[14C]carboxylic acid, choroid plexus perfusion and CSF production were measured simultaneously in rats during intraventricular administration of vasoactive intestinal polypeptide, which resulted in a decrease in CSF production of up to 30%, yet a choroid plexus perfusion increase by 20%.[48] Finally, in anesthetized rabbits, it was reported that administration of acetazolamide, a carbonic anhydrase inhibitor and potent vasodilator, yielded an approximately two-fold increase in choroid plexus perfusion but a large $55 \pm 5\%$ decrease in CSF production.[49]

These findings collectively highlight that changes in choroid plexus perfusion may or may not be directly related to CSF production activity. It is also clear that the mechanism of vasodilatory or vasoconstrictive action influences the coupling or uncoupling of CSF flow activity with choroid plexus perfusion, and it remains unclear how the study procedures which are often highly invasive and may initiate feedback processes themselves, the impact of the anesthesia, and the administration procedure (e.g. intrathecal or otherwise) additionally influence choroid plexus behavior. It should be noted that we observed a significant change in choroid plexus perfusion after surgery, however no significant change in total brain CSF volumes.

Limitations

The study should also be considered in light of several limitations. First, the population studied here is complex, suffering from a frequently aggressive arterial steno-occlusive disease that can be progressive even over the duration of this study (6–12 months for most patients). Therefore, improvements in flow that may present near the revascularization site could be offset in some patients by reduced flow in other regions. The advantage of this population is that they receive clinically indicated anastomoses procedures, which allows for the change in CSF flow and production to be measured in similar participants following an intervention that improves arterial compliance and most likely associated arterial paravascular flow. To address this limitation, we also enrolled separate patients with same diagnosis for the control group, but these patients did not receive interval surgeries. Second, we do not measure arterial paravascular flow directly, which to our knowledge has not been performed in animals or humans due to inadequacy of available methods. Rather the improvement in perfusion associated with neovascularization was reported. Importantly, the indirect revascularization procedures evaluated are not direct bypass procedures, but rather are intended to promote neoangiogenesis through dural synangiosis. Therefore, it is likely that arterial paravascular space is directly affected as new arterioles are introduced over the scan interval. Third, the comparator cohort used in this study was a similar population of patients with moyamoya but without interval surgeries. It is possible that progression will occur in this cohort as well, and, as can be seen from Figure 4, the trend for a reduction in cortical perfusion is likely a result of progressive arterial steno-occlusion. We chose this cohort to allow for direct comparison with the surgical cohort, and it should be noted that longitudinal studies of tissue volume and perfusion have been conducted in the literature to great extents, and it is largely accepted that significant changes in perfusion and CSF volume do

not occur in a cohort of this age (approximately average age of 41 years) over a relatively short duration of approximately one year.[50,51] Finally, it is well-known that delays in blood water arrival in arterial spin labeling experiments, beyond the post-labeling delay (typical range: 1500–2000 ms)[32] and arterial blood water T_1 (3.0 T $T_1 = 1650$ ms)[52] will lead to labeled blood water that remains in the arterial compartment prior to exchange with tissue water. As the choroid plexus complexes are partly perfused by the posterior circulation (e.g. posterior choroidal arteries, which branch from the posterior cerebral arteries), and the posterior circulation is largely preserved in moyamoya patients until very late disease stages, endovascular signal artifacts are low in the choroid plexus relative to more distal cortex that is perfused by the anterior circulation. In this study, we have refrained from over-interpreting quantitative perfusion values themselves due to this possibility, and this effect has been well-characterized in the literature in this population.[26,27]

In conclusion, we investigated how intracranial CSF volume, choroid plexus perfusion, and vascular health adjust in patients following an indirect surgical revascularization procedure, which is known to improve vascular compliance and possibly paravascular flow. It was observed that following surgically induced neoangiogenesis, cortical perfusion increased as expected, and this paralleled a reduction in choroid plexus perfusion. Findings are consistent with a homeostatic mechanism whereby improved arterial health, and/or reduced ischemia, can affect choroid plexus perfusion in humans.

Funding

The author(s) disclosed receipt of the following financial support for the research, authorship, and/or publication of this article: This work was supported by National Institute of Neurological Disorders and Stroke [1R01NS07882801]; National Institute of Nursing Research [1R01NR01507901]; and National Institute of Neurological Disorders and Stroke [1R01NS097763].

Declaration of conflicting interests

The author(s) declared the following potential conflicts of interest with respect to the research, authorship, and/or publication of this article: Manus J. Donahue receives research-related support from Philips North America, the National Institute of Neurological Disorders and Stroke, the National Institute of Nursing, the National Institute of Aging and is the CEO of Biosight, LLC which provides technology consulting services. He is also a paid consultant for Global Blood Therapeutics and LymphaTouch. Daniel O. Claassen receives research support from National Institute of Neurological Disorders and Stroke (NINDS), Griffin Foundation, Michael J. Fox Foundation, and Huntington's Disease Society of America (HDSA), and pharmaceutical grant support from AbbVie, Acadia, Biogen, BMA, Cerecour, Eli Lilly, Lundbeck, Jazz Pharmaceuticals, Teva Neuroscience, Wave Life Sciences, and Vaccinex. He has received personal fees for consulting and advisory board participation from Acadia, Adamas, Lundbeck, Neurocrine, and Teva Neuroscience. These agreements have been approved by Vanderbilt University Medical Center in accordance with its conflict of interest policy.

Authors' contributions

SJ: conception and design of the study, acquisition and analysis of data, drafting a significant portion of the manuscript.
CDM: conception and design of the study, acquisition and analysis of data, drafting a significant portion of the manuscript.
SKL: acquisition and analysis of data, drafting a significant portion of the manuscript.
MRJ: acquisition and analysis of data, drafting a significant portion of the manuscript.
MF: assistance with experimental procedure, revising a significant portion of the manuscript.
RC: assistance with experimental procedure, revising a significant portion of the manuscript.
PCD: assistance with experimental procedure, revising a significant portion of the manuscript.
DOC: drafting a significant portion of the manuscript.
MJD: conception and design of the study, acquisition and analysis of data, drafting a significant portion of the manuscript.

References

1. Sakka L, Coll G and Chazal J. Anatomy and physiology of cerebrospinal fluid. *Eur Ann Otorhinolaryngol Head Neck Dis* 2011; 128: 309–316.
2. Guyton AC and Hall JE. *Textbook of medical physiology*. 11th ed. Philadelphia: Elsevier Saunders, 2006.
3. Emerich DF, Vasconcellos AV, Elliott RB, et al. The choroid plexus: function, pathology and therapeutic potential of its transplantation. *Expert Opin Biol Ther* 2004; 4: 1191–1201.
4. Faraci FM, Mayhan WG and Heistad DD. Effect of serotonin on blood flow to the choroid plexus. *Brain Res* 1989; 478: 121–126.
5. Wiesmann M, Yousry I, Seelos KC, et al. Identification and anatomic description of the anterior choroidal artery by use of 3D-TOF source and 3D-CISS MR imaging. *AJNR Am J Neuroradiol* 2001; 22: 305–310.
6. Zhao L and Alsop D. Characterizing perfusion and arterial transit time of the choroid plexus with arterial spin labeling. Paris, France: International Society for Magnetic Resonance in Medicine, 2018.
7. Kaur C, Rathnasamy G and Ling EA. The choroid plexus in healthy and diseased brain. *J Neuropathol Exp Neurol* 2016; 75: 198–213.
8. Iliff JJ, Chen MJ, Plog BA, et al. Impairment of glymphatic pathway function promotes tau pathology after traumatic brain injury. *J Neurosci* 2014; 34: 16180–16193.
9. Iliff JJ and Nedergaard M. Is there a cerebral lymphatic system? *Stroke* 2013; 44(6)Suppl 1): S93–95.

10. Louveau A, Plog BA, Antila S, et al. Understanding the functions and relationships of the glymphatic system and meningeal lymphatics. *J Clin Invest* 2017; 127: 3210–3219.
11. Jessen NA, Munk AS, Lundgaard I, et al. The glymphatic system: a beginner's guide. *Neurochem Res* 2015; 40: 2583–2599.
12. Bakker EN, Bacskai BJ, Arbel-Ornath M, et al. Lymphatic clearance of the brain: perivascular, paravascular and significance for neurodegenerative diseases. *Cell Mol Neurobiol* 2016; 36: 181–194.
13. Hladky SB and Barrand MA. Mechanisms of fluid movement into, through and out of the brain: evaluation of the evidence. *Fluids Barriers CNS* 2014; 11: 26.
14. Spector R, Robert Snodgrass S and Johanson CE. A balanced view of the cerebrospinal fluid composition and functions: focus on adult humans. *Exp Neurol* 2015; 273: 57–68.
15. Iliff JJ, Wang M, Liao Y, et al. A paravascular pathway facilitates CSF flow through the brain parenchyma and the clearance of interstitial solutes, including amyloid beta. *Sci Transl Med* 2012; 4: 147ra111.
16. Absinta M, Ha SK, Nair G, et al. Human and nonhuman primate meninges harbor lymphatic vessels that can be visualized noninvasively by MRI. *Elife* 2017; 6: e29738.
17. Goulay R, Flament J, Gauberti M, et al. Subarachnoid hemorrhage severely impairs brain parenchymal cerebrospinal fluid circulation in nonhuman primate. *Stroke* 2017; 48: 2301–2305.
18. Kuroda S and Houkin K. Moyamoya disease: current concepts and future perspectives. *Lancet Neurol* 2008; 7: 1056–1066.
19. Donahue MJ, Achten E, Cogswell PM, et al. Consensus statement on current and emerging methods for the diagnosis and evaluation of cerebrovascular disease. *J Cereb Blood Flow Metab* 2018; 38: 1391–1417.
20. Hendrikse J, Petersen ET and Golay X. Vascular disorders: insights from arterial spin labeling. *Neuroimag Clin N Am* 2012; 22: 259–69, x–xi.
21. Donahue MJ, Achten E, Cogswell PM, et al. Consensus statement on current and emerging methods for the diagnosis and evaluation of cerebrovascular disease. *J Cereb Blood Flow Metab* 2018; 38: 1391–1417.
22. Dai W, Garcia D, de Bazelaire C, et al. Continuous flow-driven inversion for arterial spin labeling using pulsed radio frequency and gradient fields. *Magnet Reson Med* 2008; 60: 1488–1497.
23. Chen Y, Wolk DA, Reddin JS, et al. Voxel-level comparison of arterial spin-labeled perfusion MRI and FDG-PET in Alzheimer disease. *Neurology* 2011; 77: 1977–1985.
24. Blicher JU, Stagg CJ, O'Shea J, et al. Visualization of altered neurovascular coupling in chronic stroke patients using multimodal functional MRI. *J Cereb Blood Flow Metab* 2012; 32: 2044–2054.
25. Ances BM, McGarvey ML, Abrahams JM, et al. Continuous arterial spin labeled perfusion magnetic resonance imaging in patients before and after carotid endarterectomy. *J Neuroimaging* 2004; 14: 133–138.
26. Roach BA, Donahue MJ, Davis LT, et al. Interrogating the functional correlates of collateralization in patients with intracranial stenosis using multimodal hemodynamic imaging. *AJNR Am J Neuroradiol* 2016; 37: 1132–1138.
27. Fan AP, Guo J, Khalighi MM, et al. Long-delay arterial spin labeling provides more accurate cerebral blood flow measurements in moyamoya patients: a simultaneous positron emission tomography/MRI study. *Stroke* 2017; 48: 2441–2449.
28. Waddle SL, Juttukonda MR, Lants SK, et al. Classifying intracranial stenosis disease severity from functional MRI data using machine learning. *J Cereb Blood Flow Metab*. Epub ahead of print 8 May 2019. DOI: 10.1177/0271678X19848098.
29. Bryan RN, Cai J, Burke G, et al. Prevalence and anatomic characteristics of infarct-like lesions on MR images of middle-aged adults: the atherosclerosis risk in communities study. *AJNR Am J Neuroradiol* 1999; 20: 1273–1280.
30. Casella JF, King AA, Barton B, et al. Design of the silent cerebral infarct transfusion (SIT) trial. *Pediatr Hematol Oncol* 2010; 27: 69–89.
31. Zhang Y, Brady M and Smith S. Segmentation of brain MR images through a hidden Markov random field model and the expectation-maximization algorithm. *IEEE Transac Med Imag* 2001; 20: 45–57.
32. Alsop DC, Detre JA, Golay X, et al. Recommended implementation of arterial spin-labeled perfusion MRI for clinical applications: a consensus of the ISMRM perfusion study group and the European consortium for ASL in dementia. *Magnet Reson Med* 2015; 73: 102–116.
33. Grabner G, Janke AL, Budge MM, et al. Symmetric atlasing and model based segmentation: an application to the hippocampus in older adults. *Med Image Comput Comput Assist Intervent* 2006; 9(Pt 2): 58–66.
34. Mokri B. The Monro-Kellie hypothesis: applications in CSF volume depletion. *Neurology* 2001; 56: 1746–1748.
35. Watchmaker JM, Frederick BD, Fusco MR, et al. Clinical use of cerebrovascular compliance imaging to evaluate revascularization in patients with moyamoya. *Neurosurgery* 2019; 84: 261–271.
36. Watts R, Steinklein JM, Waldman L, et al. Measuring glymphatic flow in man using quantitative contrast-enhanced MRI. *AJNR Am J Neuroradiol* 2019; 40: 648–651.
37. Klempt ND, Sirimanne E, Gunn AJ, et al. Hypoxia-ischemia induces transforming growth factor beta 1 mRNA in the infant rat brain. *Brain Res Mol Brain Res* 1992; 13: 93–101.
38. Knuckey NW, Finch P, Palm DE, et al. Differential neuronal and astrocytic expression of transforming growth factor beta isoforms in rat hippocampus following transient forebrain ischemia. *Brain Res Mol Brain Res* 1996; 40: 1–14.
39. Chodobski A and Szmydynger-Chodobska J. Choroid plexus: target for polypeptides and site of their synthesis. *Microsc Res Tech* 2001; 52: 65–82.
40. Prehn JH, Bindokas VP, Marcuccilli CJ, et al. Regulation of neuronal Bcl2 protein expression and calcium homeostasis by transforming growth factor type beta confers

wide-ranging protection on rat hippocampal neurons. *Proc Natl Acad Sci U S A* 1994; 91: 12599–12603.
41. Yeh SJ, Tang SC, Tsai LK, et al. Ultrasonographic changes after indirect revascularization surgery in pediatric patients with moyamoya disease. *Ultrasound Med Biol* 2016; 42: 2844–2851.
42. Ogawa S, Ogata T, Shimada H, et al. Acceleration of blood flow as an indicator of improved hemodynamics after indirect bypass surgery in Moyamoya disease. *Clin Neurol Neurosurg* 2017; 160: 92–95.
43. Hua J, Donahue MJ, Zhao JM, et al. Magnetization transfer enhanced vascular-space-occupancy (MT-VASO) functional MRI. *Magn Reson Med* 2009; 61: 944–51.
44. Donahue MJ, Blicher JU, Ostergaard L, et al. Cerebral blood flow, blood volume, and oxygen metabolism dynamics in human visual and motor cortex as measured by whole-brain multi-modal magnetic resonance imaging. *J Cereb Blood Flow Metab* 2009; 29: 1856–1866.
45. Maktabi MA, Stachovic GC and Faraci FM. Angiotensin II decreases the rate of production of cerebrospinal fluid. *Brain Res* 1993; 606: 44–49.
46. Faraci FM, Mayhan WG and Heistad DD. Effect of vasopressin on production of cerebrospinal fluid: possible role of vasopressin (V1)-receptors. *Am J Physiol* 1990; 258(1 Pt 2): R94–98.
47. Schalk KA, Faraci FM, Williams JL, et al. Effect of atriopeptin on production of cerebrospinal fluid. *J Cereb Blood Flow Metab* 1992; 12: 691–696.
48. Nilsson C, Lindvall-Axelsson M and Owman C. Simultaneous and continuous measurement of choroid plexus blood flow and cerebrospinal fluid production: effects of vasoactive intestinal polypeptide. *J Cereb Blood Flow Metab* 1991; 11: 861–867.
49. Faraci FM, Mayhan WG and Heistad DD. Vascular effects of acetazolamide on the choroid plexus. *J Pharmacol Exp Ther* 1990; 254: 23–27.
50. Claassen DO, Dobolyi DG, Isaacs DA, et al. Linear and curvilinear trajectories of cortical loss with advancing age and disease duration in Parkinson's disease. *Aging Dis* 2016; 7: 220–229.
51. Donahue MJ, Faraco CC, Strother MK, et al. Bolus arrival time and cerebral blood flow responses to hypercarbia. *J Cereb Blood Flow Metab* 2014; 34: 1243–1252.
52. Lu H, Clingman C, Golay X, et al. Determining the longitudinal relaxation time (T1) of blood at 3.0 Tesla. *Magn Reson Med* 2004; 52: 679–682.